Competition between Allowed and First-Forbidden β Decay: The Case of ^{208}Hg $\rightarrow$ ^{208}Tl

R. J. Carroll,[1] Zs. Podolyák,[1,2] T. Berry,[1] H. Grawe,[3] T. Alexander,[1] A. N. Andreyev,[4,22] S. Ansari,[5] M. J. G. Borge,[6] M. Brunet,[1] J. R. Creswell,[7] L. M. Fraile,[8] C. Fahlander,[9] H. O. U. Fynbo,[10] E. R. Gamba,[11] W. Gelletly,[1] R.-B. Gerst,[5] M. Górska,[3] A. Gredley,[7] P. T. Greenlees,[12,13] L. J. Harkness-Brennan,[7] M. Huyse,[14] S. M. Judge,[15] D. S. Judson,[7] J. Konki,[12,13] J. Kurcewicz,[6] I. Kuti,[16] S. Lalkovski,[1] I. H. Lazarus,[17] R. Lică,[6,18] M. Lund,[10] M. Madurga,[6,23] N. Marginean,[18] R. Marginean,[18] I. Marroquin,[19] C. Mihai,[18] R. E. Mihai,[18] E. Nácher,[19] A. Negret,[18] C. Nita,[18,11] S. Pascu,[18] R. D. Page,[7] Z. Patel,[1] A. Perea,[19] J. Phrompao,[20] M. Piersa,[21] V. Pucknell,[17] P. Rahkila,[12,13] E. Rapisarda,[6] P. H. Regan,[1,15] F. Rotaru,[18] M. Rudigier,[1] C. M. Shand,[1] R. Shearman,[1,15] S. Stegemann,[5] T. Stora,[6] Ch. Sotty,[14,18] O. Tengblad,[19] P. Van Duppen,[14] V. Vedia,[8] R. Wadsworth,[4] P. M. Walker,[1] N. Warr,[5] F. Wearing,[7] and H. De Witte[14]

[1]*Department of Physics, University of Surrey, Guildford GU2 7XH, United Kingdom*
[2]*ExtreMe Matter Institute EMMI, GSI Helmholtzzentrum für Schwerionenforschung, Planckstrasse 1, 64291 Darmstadt, Germany*
[3]*GSI Helmholtzzentrum für Schwerionenforschung GmbH, Planckstrasse 1, 64291 Darmstadt, Germany*
[4]*University of York, Dept Phys, North Yorkshire YO10 5DD, United Kingdom*
[5]*Institut für Kernphysik der Universität zu Köln, Zülpicher Str. 77, 50937 Köln, Germany*
[6]*CERN, Physics Department, 1211 Geneva 23, Switzerland*
[7]*Department of Physics, Oliver Lodge Laboratory, University of Liverpool, Liverpool L69 7ZE, United Kingdom*
[8]*Grupo de Física Nuclear & IPARCOS, Universidad Complutense de Madrid, CEI Moncloa, E-28040 Madrid, Spain*
[9]*Department of Physics, Lund University, S-22100 Lund, Sweden*
[10]*Department of Physics and Astronomy, Aarhus University, DK-8000 Aarhus, Denmark*
[11]*University of Brighton, Brighton BN2 4GJ, United Kingdom*
[12]*University of Jyvaskyla, Department of Physics, University of Jyvaskyla, P.O. Box 35, FI-40014 Jyvaskyla, Finland*
[13]*Helsinki Institute of Physics, University of Helsinki, P.O. Box 64, FI-00014 Helsinki, Finland*
[14]*KU Leuven, Instituut voor Kern- en Stralingsfysica, Celestijnenlaan 200D, 3001 Leuven, Belgium*
[15]*National Physical Laboratory, Teddington, Middlesex TW11 0LW, United Kingdom*
[16]*Institute of Nuclear Research of the Hungarian Academy of Sciences, 4026 Debrecen, Hungary*
[17]*STFC, Daresbury Laboratory, Warrington WA4 4AD, United Kingdom*
[18]*Horea Hulubei National Institute for Physics and Nuclear Engineering, RO-077125 Bucharest, Romania*
[19]*Instituto de Estructura de la Materia, CSIC, Serrano 113 bis, E-28006 Madrid, Spain*
[20]*Department of Physics and Materials Science, Chiang Mai University, 50200 Chiang Mai, Thailand*
[21]*Faculty of Physics, University of Warsaw, PL 02-093 Warsaw, Poland*
[22]*Advanced Science Research Center, Japan Atomic Energy Agency, Tokai-mura, Ibaraki 319-1195, Japan*
[23]*Department of Physics and Astronomy, University of Tennessee, Knoxville, Tennessee 37996, USA*

The β decay of ^{208}Hg into the one-proton hole, one neutron-particle $^{208}_{81}$Tl$_{127}$ nucleus was investigated at CERN-ISOLDE. Shell-model calculations describe well the level scheme deduced, validating the proton-neutron interactions used, with implications for the whole of the $N > 126$, $Z < 82$ quadrant of neutron-rich nuclei. While both negative and positive parity states with spin 0 and 1 are expected within the Q_β window, only three negative parity states are populated directly in the β decay. The data provide a unique test of the competition between allowed Gamow-Teller and Fermi, and first-forbidden β decays, essential for the understanding of the nucleosynthesis of heavy nuclei in the rapid neutron capture process. Furthermore, the observation of the parity changing $0^+ \rightarrow 0^- \beta$ decay where the daughter state is core excited is unique, and can provide information on mesonic corrections of effective operators.

Introduction.—Shell structure naturally arises for interacting multiparticle quantum systems. The concept has been successfully used in atomic physics [1], nuclear physics [2], and for metallic clusters [3]. In the case of atomic nuclei, the neutron magic numbers play an essential role in the nucleosynthesis of elements heavier than iron. Both in the slow (*s*) and rapid (*r*) neutron-capture processes

the abundances of nuclei with magic neutron numbers are enhanced. Thus the $A \sim 195$ r-process abundance peak is the consequence of the $N = 126$ neutron shell closure. β-decay half-lives are basic nuclear physics input in r-process calculations. While half-lives of a large number of fission products were recently measured [4,5], the $N = 126$ r-process path nuclei are experimentally unreachable [6,7], and we have to rely on theoretical calculations. In this context the nuclei in the $N = 126$ region are of particular interest [8] because first-forbidden (FF) β decays successfully compete [9–15] with allowed Gamow-Teller (GT) and Fermi decays, and this impacts on the calculations of r-process nucleosynthesis abundances [16]. However, the calculation of FF β decay is notoriously difficult and subject to debate.

An ideal nucleus to study the competition between FF and allowed β decay should have a small number of both negative and positive parity levels below the Q_β value, with simple and well-understood wave functions. The β decay of ^{208}Hg into the one-proton-hole, one-neutron-particle ^{208}Tl nucleus with a $Q_\beta = 3.48$ (3) MeV [17] provides this ideal testing ground. Q_β is low due to the vicinity of the stability line, and the wave functions are simple due to the small number of valence nucleons outside the doubly magic ^{208}Pb core. Furthermore, states with spin $I = 0$ and $I = 1$ of both positive and negative parities are available by combining a neutron above the $N = 126$ core with a proton hole below $Z = 82$. In addition, ^{208}Tl, with one proton hole and one neutron outside ^{208}Pb, provides directly the neutron-proton two-body matrix elements for the shell-model calculations [18]. Therefore the understanding of excited states in ^{208}Tl is essential for the successful prediction of properties of nuclei in the little studied $N > 126$, $Z < 82$ region [19]. In this region excited states were observed in only a handful of nuclei: ^{208}Tl [20] and ^{209}Tl [21–23], and more recently, with the advent of radioactive-beam facilities, γ-ray spectroscopy following internal decays provided information on the yrast structures of ^{208}Hg [24], ^{209}Tl [24], and ^{210}Hg [25]. Single-neutron states in ^{207}Hg [26] and γ-ray transitions in ^{211,213}Tl [27] were also identified.

In this Letter we present results from the β decay of ^{208}Hg into ^{208}Tl, providing information on the competition between allowed and first-forbidden β decay and validating the proton-neutron interaction "south-east" of ^{208}Pb.

Experimental details.—Experiments to measure the β decay of ^{208}Hg to ^{208}Tl were performed at the ISOLDE decay station (IDS) at CERN. ^{208}Hg nuclei were produced by impinging 1.4 GeV protons on a molten lead target. These were extracted using a FEBIAD VADIS ion source [28], accelerated to 30–50 keV, mass selected with a dipole magnet, and finally implanted in a tape at the IDS. Two experiments were performed [29] in 2014 and 2016. In both cases the IDS consisted of plastic scintillation detectors for β-particle detection surrounding the implantation point, and five composite Ge detectors for γ-ray measurements. In 2014
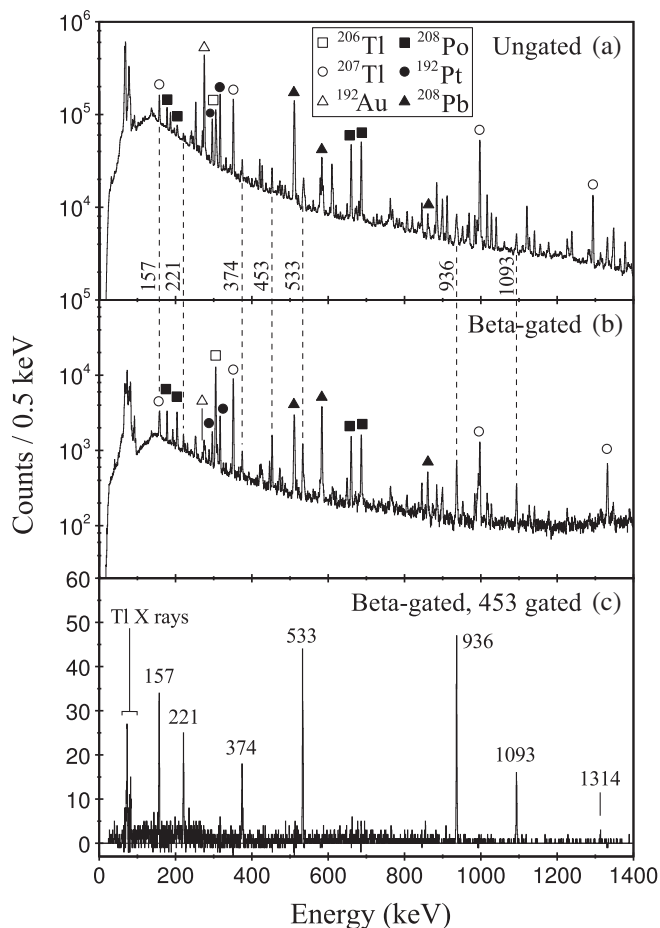

FIG. 1. (a) γ-ray spectrum measured at the implantation position. Daughter nuclei are indicated. The transmission of $A = 208$ molecules ^{206}Hg^{1}H$_2$ and ^{192}Au^{16}O resulted in transitions in ^{206}Tl, ^{192}Pt, and ^{192}Au. Some ^{207}Hg, decaying into ^{207}Tl was also transmitted. (b) β-gated spectrum. (c) β-gated spectrum in coincidence with a 453 keV γ-ray transition, providing a clean ^{208}Tl spectrum.

four Clover Ge and one Miniball Cluster detector were used, while in 2016 five clover Ge detectors were employed. The γ-ray detection efficiency at 1 MeV was 8% and 4% in 2014 and 2016. The β-particle detection efficiencies were $\sim$30% in 2014 and $\sim$85% (with a $\sim 4\pi$ detector placed in the vacuum chamber) in 2016. Data were time stamped to a precision of 10 ns and recorded using a triggerless data acquisition system. Correlations between detectors were made in software using the GRAIN software package [30].

Results.—The rate of ^{208}Hg delivery to the implantation position was $\sim$5 and 25 Hz in 2014 and 2016, respectively. Better statistics on the ^{208}Hg $\rightarrow$ ^{208}Tl decay were obtained in 2016, although the data were dominated by the β decays of ^{208}At to ^{208}Po [31]. The 2014 data were cleaner, so the spectra presented here are from the 2014 measurement, while the intensities and lifetimes are from 2016. γ-ray spectra, with and without β coincidence requirements, are shown on Fig. 1. By selecting the well-established 453 keV
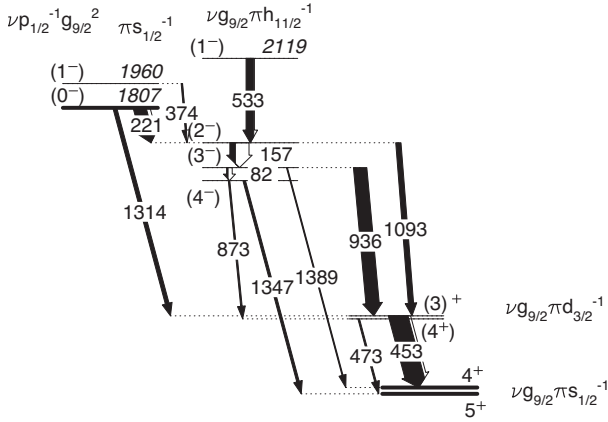
FIG. 2. Proposed level scheme of ^{208}Tl from the present work. The long-lived states are in bold. The widths of the arrows represent the transition intensity, with the black and white parts corresponding to the γ and conversion electon emmissions, respectively. The dominant configurations are indicated.

γ ray in ^{208}Tl [20], the coincidence spectrum presented in Fig. 1(c) is clean, showing the 72 and 82 keV K_α and K_β thallium x rays and a small number of γ rays. Based on $\gamma - \gamma$ coincidences the level scheme of ^{208}Tl was obtained and it is given in Fig. 2. The properties of the γ-ray transitions assigned to ^{208}Tl are listed in Table I.

The ^{208}Tl level scheme deduced is in agreement with the one obtained following the α decay of ^{212}Bi [20]. The spin parities of the 5^+ ground state, the 4^+ 40, the (4^+) 473, and the $(3)^+$ 493 keV excited states are adopted from these works. The rest of the level scheme is new. We do not confirm the level scheme presented following a previous β-decay study, where ^{208}Hg was produced in multinucleon reactions followed by chemical separation [33,34].

Almost all of the γ rays assigned to ^{208}Tl are in prompt coincidence with β particles. The exceptions are the 221 and 1314 keV transitions originating from the excited state at 1807 keV. By examining the β–γ time spectrum, shown in Fig. 3, a lifetime of $T_{1/2} = 1.3(1)$ μs was obtained for the 1807 keV level.

By comparing the intensity of the 453 keV $M1$ transition with that of the 157 keV in the 936 keV gated spectrum, the electron conversion coefficient of the 157 keV line was obtained as $\alpha = 2.1(3)$. This proves its M1 character [$\alpha_{\text{theor}}(M1) = 2.38$ [35]]. Consequently, the excited states at 1429 and 1586 keV have the same parity. In addition, the sum (γ plus conversion electron) intensity of the 221, 1314, 374, and 533 keV transitions cannot be larger than the total intensity reaching the ground state. This requires that the electron conversion coefficients of all the above listed γ rays are small. This rules out $M1$ character for the 221 keV transition [$\alpha_{\text{theor}}(M1) = 0.92$ [35]]. $E2$ is favored by the isomerism as $E1$ yields the extreme hindrance of 10^{-8} W.u..

Two rather different values have been published for the lifetime of the ^{208}Hg ground state. $T_{1/2} = 41^{+5}_{-4}$ min was

TABLE I. Properties of the γ rays in ^{208}Tl observed following β decays of ^{208}Hg. Shell-model transition strengths are indicated. The theoretical γ-ray branching ratios, obtained by using experimental transition energies, are compared with the experimental ones. The energies of *nonobserved* γ rays for which transition strengths are calculated are given in italics. For the dominant configurations of the individual states see Fig. 2.

E_i (keV)	E_γ (keV)	$BR_{\gamma Expt}$ %	$I_i^\pi \to I_f^\pi$	σL	$B(\sigma L)_{\text{theor}}$ (W.u.)	$BR_{\gamma \text{theor}}$ (%)
40	39.858(4)[a]	100	$4_1^+ \to 5_1^+$	M1	1.15	100
				E2	0.33	
473	433.7(5)[b]	25(5)[b]	$4_2^+ \to 4_1^+$	M1	0.029	9
				E2		0.51
	473(1)	75(5)	$\to 5_1^+$	M1	0.12	91
				E2		1.39
493	452.8(2)	100	$3_1^+ \to 4_1^+$	M1	0.017	95
				E2	0.40	
	493	...	$\to 5_1^+$	E2	2.26	5
1347	873(1)	35(14)	$4_1^- \to 4_2^+$	E1	...	
	1347.1(4)	65(22)	$\to 5_1^+$	E1	...	
	...	...	$\to 5_1^-$	M1	4.18	
				E2	3.31	
1429	82(1)[c]	7(2)[c]	$3_1^- \to 4_1^-$	M1	4.45	
				E2	2.31	
	936.3(2)	86(9)	$\to 3_1^+$	E1	...	
	1389.3(5)	7(2)	$\to 4_1^+$	E1	...	
			$\to 4_2^+$	E1	...	
1586	157.0(4)	48(11)	$2_1^- \to 3_1^-$	M1	4.88	100
				E2	1.10	
	239		$\to 4_1^-$	E2	0.011	0
	1093.3(3)	52(7)	$\to 3_1^+$	E1	...	
1807	220.7(2)	74(11)	$0_1^- \to 2_1^-$	E2	0.0018	34
	1314.0(3)	26(4)	$\to 3_1^+$	E3	0.0079	66
1960	374(1)	100	$1_1^- \to 2_1^-$	M1	0.054	82
				E2	0.00015	
	154	...	$\to 0_1^-$	M1	0.17	18
	531	...	$\to 3_1^-$	E2	0.0019	0
2119	533.0(2)	100	$1_2^- \to 2_1^-$	M1	4.26	100
				E2	0.52	
	313	...	$\to 0_1^-$	M1	0.0044	0
	690	...	$\to 3_1^-$	E2	0.039	0

[a]Unobserved in the present experiment. From Ref. [20].
[b]Unobserved in the present experiment. From Refs. [20,32].
[c]Unobserved transition. Its existence deduced from γ-γ coincidence analysis.

reported from the earlier mentioned β-decay measurements [36,37], but recently a much shorter value of 132(50) s was published following a projectile fragmentation experiment [7,38]. We measured the half-life by implanting ^{208}Hg nuclei for a fixed time, than observing their decay. After removing the activity with the tape system, we repeated this sequence several times. In our first experiment in 2014 we aimed to be sensitive to 30 min lifetime. The nonobservation of the ^{208}Hg decay indicated that its lifetime is much shorter than 30 min. In 2016, we measured the half-life
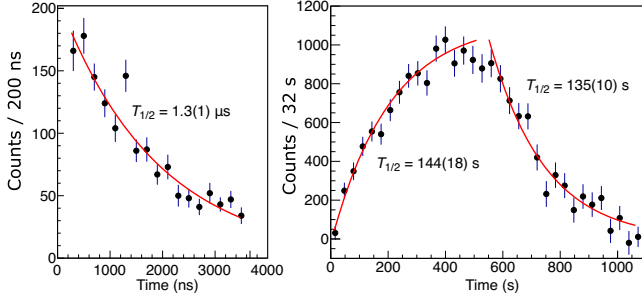
FIG. 3. (a) Lifetime of the isomeric state at $E_x = 1807$ keV in ^{208}Tl. The time difference between the β particle and any of the 221–453 and 221–936 keV γ-ray pairs is shown. (b) Lifetime of the ^{208}Hg ground state determined both from the accumulation and decay phases. Since the former one assumes a constant implantation rate, the value obtained during the exponential decay phase is adopted.
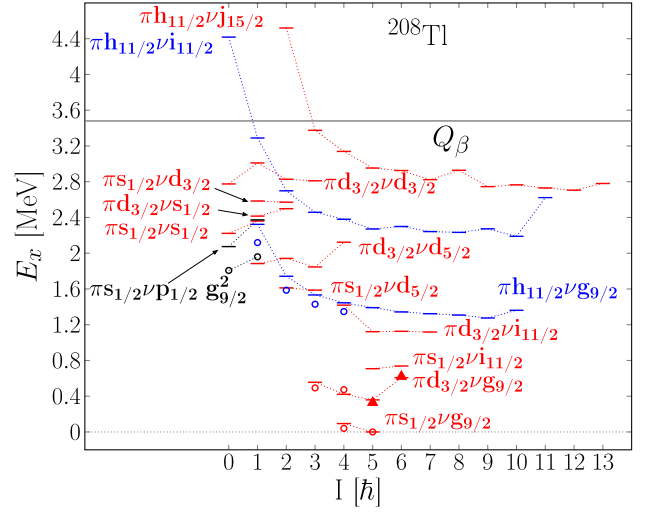

FIG. 4. Comparison of experimentally observed states with shell-model calculations. The horizontal lines indicate the theoretical values. The experimental values are denoted by circles (for states observed in the present experiment) and triangles (states from Ref. [20]). Levels with the same dominant configurations are connected. Positive (negative) parity states are shown in red (blue). Black is used for core-excited negative-parity states.

of ^{208}Hg, from the time profile shown in Fig. 3, to be $T_{1/2} = 135(10)$ s. This is in good agreement and more accurate than the recently reported value obtained at GSI. We used our new lifetime value for the log ft calculations.

The spin parities of the excited states are restricted by β-decay considerations. There are three directly fed states at 2119, 1960, and 1807 keV with relative feedings of 25(4)%, 8(3)%, and 66(5)%. The corresponding log ft values are 5.3(1), 6.0(2), 5.2(1), respectively. This restricts the spin of these states to 0 or 1, based on the log ft systematics of Ref. [39]. Lower-lying levels need to have increasing spins as they decay towards the 5^+ ground state. Ultimately the spin parities of the three states fed directly in β decay are assigned by comparison with shell-model calculations.

Discussion.—In order to understand the structure of ^{208}Tl, shell model calculations have been performed, using the OXBASH [40] code. Level energies and transition rates were calculated in the $\pi(0g_{7/2}, 1d, 2s_{1/2}, 0h_{11/2})$ $\nu(0i_{11/2}, 1g, 2d, 3s_{1/2}, 0j_{15/2})$ model space using the Kuo-Herling interaction [41] for $\pi\pi$ and $\nu\nu$ and H7B [42] for $\pi\nu$. For ^{208}Tl this reduces to H7B only. The calculations were done in particle-particle mode relative to a hypothetical ^{132}Sn core. In an extended model space neutron particle–hole (ph) excitations from the $2p_{1/2}$ and $2p_{3/2}$ orbits across the $N = 126$ shell closure were considered to account for the $2p2h$ content in the $(0-1)^-$ states and γ-ray transitions between them. The other transitions were calculated in the valence space only. The inclusion of the core breaking excitation is needed in order to account for the $1/2^-$ state with $\nu p_{1/2}^{-1}\nu g_{9/2}^2$ configuration at the relatively low energy of 2149 keV in ^{209}Pb [23]. γ-decay transition rates were calculated using effective operators $e_\pi = 1.5e$, $e_\nu = 0.85e$ for $E2$ transitions and $g_s = 0.7g_s^{\text{free}}$ for $M1$ transitions. No $E1$ transitions are allowed in this model space.

In ^{208}Tl, the level density is rather low at low excitation energies. Figure 4 shows the theoretical level scheme featuring relevant states with leading ph configuration

$\nu(g_{9/2}, i_{11/2}, s, d)$ $\pi(s, d)$ and $\nu j_{15/2}\pi h_{11/2}$ for even parity and $\nu(g_{9/2}, i_{11/2})$ $\pi h_{11/2}$ for odd parity below the Q_β value. In addition, the core excited $2p2h$ $I^\pi = (0, 1)^-$ $\pi s_{1/2}^{-1}\nu g_{9/2}^2 p_{1/2}^{-1}$ states are also shown. Note that the used model space does not allow for the prediction of collective octupole states [43,44]. These are negative parity states with spin parities ranging from 1^- $(4^+ \otimes 3^-)$ to 8^- $(5^+ \otimes 3^-)$, expected (at $\sim$2.6 MeV) several hundreds of keV above the highest level observed here.

The calculations indicate that the only possible isomer at $\approx$2 MeV excitation energy is the 0^- state with $\nu p_{1/2}^{-1}g_{9/2}^2\pi s_{1/2}^{-1}$ character. Accordingly we associate this with the 1807 keV level. The other member of the multiplet is predicted to be the lowest lying 1^- state, therefore we assign this to the 1960 keV state. These assignments are supported by a comparison to the ^{206}Tl ground state and 305 keV excited state with hh configuration $\nu p_{1/2}^{-1}\pi s_{1/2}^{-1}$. The ^{208}Tl states have the structure $^{208}\text{Tl}_{(0,1)^-} = {^{206}\text{Tl}}_{(0,1)^-} \times {^{210}\text{Pb}}_{0^+}$. This manifests itself in similar log ft values in ^{206,208}Hg β decays, namely, 5.41(6) and 5.24(10) in ^{206}Tl $I^\pi = 0^-, 1^-$ [45] vs 5.2(1) and 6.0(2) in the ^{208}Tl analogs. The relatively low excitation energy of the core excited states in ^{208}Tl is readily explained by the strong $\nu g_{9/2}^2$ pairing which partially compensates the $N = 126$ shell gap.

The configurations of the low-energy states, below 1 MeV, are established as given on Fig. 4. We associate the 2119, 1586, 1429, and 1347 keV levels with the 1^--4^- members of the $\nu g_{9/2}\pi h_{11/2}^{-1}$ multiplet. As expected, these states are connected by strong $M1$ transitions, with decreasing energies. These compete with weak, but high-energy $E1$ transitions.

There is good agreement between the experimental and theoretical level schemes (see Fig. 4). The small discrepancy for negative parity states is due to omission of the octupole phonon coupled to the low-lying positive-parity states, which by mixing would lower the energies of the yrast states. The highly retarded transition strengths of the γ rays depopulating the 0^- isomer are also well reproduced. The experimental transition strengths $B(E2) = 6.8(12) \times 10^{-3}$ and $B(E3) = 11.5(20) \times 10^{-3}$ W.u. for the 221 and 1314 keV transitions, respectively, compare well with the theoretical values of $B(E2) = 1.8 \times 10^{-3}$ and $B(E3) = 7.9 \times 10^{-3}$ W.u. The experimental branching ratios are in good agreement with the theoretical values, as shown in Table I. While the model space does not allow for $E1$ transitions, their reduced transition strengths can be estimated based on the experimental branching ratios and the theoretical $B(M1)$ and $B(E2)$ values of the competing $M1$ and $E2$ transitions. $B(E1)$ values of all observed transitions are of the order of 10^{-5}–10^{-6} W.u. All possible, but not observed $E1$ transitions have strengths of $B(E1) < 3 \times 10^{-5}$ W.u..

While we assign negative parity to all three states directly populated by β decay, we examined other scenarios. In particular we looked into the possibility that the directly populated states are of positive parity 0^+ with $\nu s_{1/2}\pi s_{1/2}^{-1}$ configuration or 1^+ with $\nu s_{1/2}\pi s_{1/2}^{-1}$, $\nu s_{1/2}\pi d_{3/2}^{-1}$, and $\nu d_{5/2}\pi d_{3/2}^{-1}$ (see Fig. 4). None of the scenarios, with the exception of that presented in Fig. 2 is compatible with the shell model calculations.

We now examine the β decay of ^{208}Hg. First-forbidden β decays populate negative parity states in ^{208}Tl. These correspond to $\nu g_{9/2} \to \pi h_{11/2}$ and $\nu i_{11/2} \to \pi h_{11/2}$ decays. The measured $\log ft$ values in the range of 5.2–6.0 are in line with those observed for first-forbidden decays in this mass region [20,46]. We refrain from a shell model calculation of rank $L = 0, 1$ FF $0^+ \to (0,1)^-$ transitions as a consistent treatment requires full inclusion of $\Delta l = 1$ $\pi\nu$ orbitals in $1p1h$ core excitations, i.e., $2p2h$ states in ^{208}Tl [47,48]. We note that the shell-model calculations available for the β decay of $N = 126$ nuclei [9,10] do not consider neutrons above the 126 shell closure, therefore cannot provide reliable estimates for the decay of ^{208}Hg.

Positive parity states could be populated by the allowed β decay. For neutrons above $N = 126$ there are neither allowed Gamow-Teller (GT) nor Fermi transitions to protons below $Z = 82$. This is because the number of nodes between the corresponding orbitals change ($\Delta n = 1$), and hence the orthogonality of the radial wave functions zeroes the GT matrix element as its operator contains no radial dependence [49,50]. Besides, the Fermi operator does not act on the radial part of the wave functions. For $N > 126$ the only allowed transition is the GT $\nu i_{11/2} \to \pi i_{13/2}$, which requires at least $1p1h$ proton core excitations. For $N < 126$ the allowed GT/Fermi

transitions are $\nu h_{9/2} \to \pi(h_{11/2}, h_{9/2})$, $\nu(f_{5/2}, f_{7/2}) \to \pi(f_{5/2}, f_{7/2})$, $\nu i_{13/2} \to \pi i_{13/2}$, and $\nu(p_{3/2}, p_{1/2}) \to \pi(p_{3/2}, p_{1/2})$. The $\nu h_{9/2} \to \pi h_{9/2}$ GT decay would populate $1p1h$ neutron core excitations at $E_x \sim 8$ MeV, higher than the aforementioned $\nu i_{11/2} \to \pi i_{13/2}$. All others need $2p2h$ core excitations, consequently lying even higher in energy, well outside the β-decay window and beyond the neutron separation energy, therefore they cannot be populated in β decay. The several 1^+ and 0^+ states expected in ^{208}Tl to lie below the Q_β value (see Fig. 4) could be mixed with the lowest same spin GT resonances. Specifically, $\pi^{-2}\pi i_{13/2}\nu i_{11/2}$ states, if mixed with the lower lying 1^+ and 0^+ configurations, could act as a "doorway" to populate them in (weak) GT, while their γ decay will proceed via their main configurations. The experimental $\log ft$ values would correspond to an estimated 1% core-excited admixture in the wave functions. The inclusion of only one-particle one-hole proton or neutron core excitation into the shell model calculations does not provide the required mixing for these decays. However, calculations including one-particle one-hole core excitations for both protons and neutrons are not feasible for ^{208}Tl.

The $FF0 \to 0$ transition, despite its unique core excited nature [51] with a $\nu(g_{9/2}^2)_{0^+}$ spectator, exhibits a $\log ft = 5.2(1)$ similar to the corresponding $p_{1/2} \leftrightarrow s_{1/2}$ transitions in ^{206}Hg $\to$ ^{206}Tl $(0^+ \to 0^-)$ and ^{206}Tl $\to$ ^{206}Pb $(0^- \to 0^+)$ [45]. This is in-line with the previously established 30% underestimate of the theoretical mesonic exchange correction [47].

In summary, the β decay of ^{208}Hg was studied. The level scheme of the single proton-hole single neutron-particle ^{208}Tl nucleus was established, providing the first direct test of the proton-neutron residual interaction in the $N > 126$, $Z < 82$ quadrant. ^{208}Hg provides a unique testing ground of the competition between allowed and first-forbidden β decay. However, with a half-life of 135(10) s, it populates directly only negative parity states via first-forbidden decays. The strongest branch establishes a $0^+ \to 0^-$ decay to a core excited daughter state. This is the first such β decay observed and provides information on meson corrections of effective operators. The present data provide important constraints on theoretical models addressing the competition between allowed and first-forbidden β decays, important for the detailed understanding of the nucleosynthesis of heavy r-process elements.

[1] N. Bohr, Philos. Mag. Ser. 5 **26**, 1 (1913).
[2] M. Goppert-Mayer, Phys. Rev. **74**, 235 (1948).
[3] O. Echt, K. Sattler, and E. Recknagel, Phys. Rev. Lett. **47**, 1121 (1981).
[4] G. Lorusso et al., Phys. Rev. Lett. **114**, 192501 (2015).
[5] J. Wu et al., Phys. Rev. Lett. **118**, 072701 (2017).
[6] A. I. Morales, J. Benlliure, T. Kurtukian-Nieto, K. H. Schmidt, S. Verma et al., Phys. Rev. Lett. **113**, 022702 (2014).
[7] R. Caballero-Folch et al., Phys. Rev. Lett. **117**, 012501 (2016).
[8] H. Grawe, K. Langanke, and G. Martìnez-Pinedo, Rep. Prog. Phys. **70**, 1525 (2007).
[9] T. Suzuki, T. Yoshida, T. Kajino, and T. Otsuka, Phys. Rev. C **85**, 015802 (2012).
[10] Q. Zhi, E. Caurier, J. J. Cuenca-Garcia, K. Langanke, G. Martinez-Pinedo, and K. Sieja, Phys. Rev. C **87**, 025803 (2013).
[11] D. L. Fang, B. A. Brown, and T. Suzuki, Phys. Rev. C **88**, 034304 (2013).
[12] T. Marketin, L. Huther, and G. Martinez-Pinedo, Phys. Rev. C **93**, 025805 (2016).
[13] P. Moller, B. Pfeiffer, and K.-L.Kratz, Phys. Rev. C **67**, 055802 (2003).
[14] H. Koura, T. Tachibana, M. Uno, and M. Yamada, Prog. Theor. Phys. **113**, 305 (2005).
[15] I. Borzov, Nucl. Phys. **A777**, 645 (2006).
[16] N. Nishimura, Z. Podolyák, D.-L. Fang, and T. Suzuki, Phys. Lett. B **756**, 273 (2016).
[17] W. J. Huang, G. Audi, M. Wang, F. G. Kondev, S. Naimi, and X. Xu, Chin. Phys. C **41**, 030002 (2017).
[18] B. A. Brown, Prog. Part. Nucl. Phys. **47**, 517 (2001).
[19] W. Korten et al., Eur. Phys. J. A **56**, 137 (2020).
[20] M. J. Martin, Nucl. Data Sheets **108**, 1583 (2007).
[21] C. Ellegaard, P. D. Barnes, and E. R. Flynn, Nucl. Phys. **A259**, 435 (1976).
[22] B. M. S. Amro, C. J. Lister, E. A. McCutchan, W. Loveland, P. Chowdhury et al., Phys. Rev. C **95**, 014330 (2017).
[23] J. Chen and F. G. Kondev, Nucl. Data Sheets **126**, 373 (2015).
[24] N. Al-Dahan et al., Phys. Rev. C **80**, 061302 (2009).
[25] A. Gottardo et al., Phys. Lett. B **725**, 292 (2013).
[26] T. L. Tang, B. P. Kay, C. R. Hoffman, J. P. Schiffer, D. K. Sharp et al., Phys. Rev. Lett. **124**, 062502 (2020).
[27] A. Gottardo et al., Phys. Rev. C **99**, 054326 (2019).
[28] T. Stora, Nucl. Instrum. Methods Phys. Res., Sect. B **317**, 402 (2013).
[29] T. Berry et al., Phys. Rev. C **101**, 054311 (2020).
[30] P. Rahkila, Nucl. Instrum. Methods Phys. Res., Sect. A **595**, 637 (2008).
[31] M. Brunet et al., J. Phys. Conf. Ser. (to be published).
[32] R. Benoit, G. Bertolini, F. Capellani, and G. Restelli, Nuovo Cimento B **49**, 125 (1967).
[33] L. Zhang, K. Morita, H. Qing-Yuan, A. Yoshida, Z. Jin-Hua, Z. Ji-Wen, L. Zhan-Kui, Y. H. Pu, H. Kudo, and Y. Yano, Chin. Phys. Lett. **20**, 1031 (2003).
[34] L. Zhang et al., Eur. Phys. J. A **16**, 299 (2003).
[35] T. Kibédi, T. W. Burrows, M. B. Trzhaskovskaya, P. M. Davidson, and C. W. Nestor, Nucl. Instrum. Methods Phys. Res., Sect. A **589**, 202 (2008).
[36] L. Zhang, Z. Jin-hua, Z. Ji-wen, W. Ji-cheng, Y. Yong-feng, Q. Zhi, and G. Tian-rui, Chin. Phys. Lett. **14**, 507 (1997).
[37] L. Zhang et al., Phys. Rev. C **49**, R592 (1994).
[38] R. Caballero-Folch et al., Phys. Rev. C **95**, 064322 (2017).
[39] B. Singh, J. L. Rodriguez, S. S. M Wong, and J. K. Tuli, Nucl. Data Sheets **84**, 487 (1998).
[40] B. A. Brown et al., OXBASH for Windows, MSU-NSCL Report No. 1289, 2004.
[41] T. T. S. Kuo and G. H. Herling, US Naval Research Laboratory Report No. 2258, 1971 (to be published).
[42] A. Hosaka, K.-I. Kubo, and H. Toki, Nucl. Phys. **A444**, 76 (1985).
[43] E. Wilson et al., Phys. Lett. B **747**, 88 (2015).
[44] Zs. Podolyák et al., J. Phys. Conf. Ser. **580**, 012010 (2015).
[45] F. G. Kondev, Nucl. Data Sheets **109**, 1527 (2008).
[46] J. Daamgard, R. Broglia, and C. Riedel, Nucl. Phys. **A135**, 310 (1969).
[47] E. K. Warburton, Phys. Rev. Lett. **66**, 1823 (1991).
[48] E. K. Warburton and I. S. Towner, Phys. Rep. **242**, 103 (1994), and references therein.
[49] T. A. Berry et al., Phys. Lett. B **793**, 271 (2019).
[50] V. M. Datar, C. V. K. Baba, S. N. Acharya, S. A. Chitambar, H. C. Jain, S. K. Bhattacherjee, and C. S Warke, Phys. Rev. C **22**, 1787 (1980).
[51] B. Singh, J. L. Rodriguez, S. S. M. Wong, and J. K. Tuli, Nucl. Data Sheets **84**, 487 (1998).